SCIENCE CHINA
Technological Sciences

• Article •

doi: 10.1007/s11431-016-0529-3

Bioinspired robust nanocomposites of cooper ions and hydroxypropyl cellulose synergistic toughening graphene oxide

ZHANG Qi[1†], WAN SiJie[1†], JIANG Lei[1] & CHENG QunFeng[1,2*]

[1] *Key Laboratory of Bio-inspired Smart Interfacial Science and Technology of Ministry of Education, School of Chemistry and Environment, Beihang University, Beijing 100191, China;*
[2] *State Key Laboratory for Modification of Chemical Fibers and Polymer Materials, Donghua University, Shanghai 201620, China*

Received July 10, 2016; accepted August 29, 2016

The hierarchical micro/nanoscale layered formation of organic and inorganic components of natural nacre, results in abundant interfacial interactions, providing an inspiration for fabricating bioinspired nanocomposites through constructing the interfacial interactions. Herein, we demonstrated the synergistic interfacial interactions of hydrogen bonding from hydroxypropyl cellulose and ionic bonding from copper ions upon the reduced graphene oxide based bioinspired nanocomposites, which show the integrated tensile strength, toughness and excellent fatigue-resistant property, as well as high electrical conductivity. These extraordinary properties allow this kind of bioinspired nanocomposites to potentially utilize in the fields of aerospace, flexible electronics devices, etc. This study also opens a door for fabricating excellent mechanical performance graphene-based bioinspired nanocomposites via synergistic interfacial interactions in the future.

bioinspired, robust, nanocomposites, synergistic toughening, cooper ions

Citation: Zhang Q, Wan S J, Jiang L, et al. Bioinspired robust nanocomposites of cooper ions and hydroxypropyl cellulose synergistic toughening graphene oxide. Sci China Tech Sci, 2016, doi: 10.1007/s11431-016-0529-3

1 Introduction

Natural nacre demonstrates the unique mechanical properties, because of its hierarchical micro/nanoscale structure and abundant interfacial interactions [1,2]. Inspired by nacre, many high performance graphene-based bioinspired nanocomposites have been fabricated via different interfacial interactions, including hydrogen bonding, such as graphene oxide (GO)-poly (methyl methacrylate) (GO-PMMA) [3], GO-(silk) (GO-SL) [4,5], GO nanosheet-poly (vinyl alcohol) (GO-PVA) [6], etc; ionic bonding including GO-Mg^{2+} [7], GO-Ca^{2+} [7], GO-Al^{3+} [8], etc; π-π interaction containing GO-polyethylene glycol (GO-PEG) [9], GO-poly (acrylic acid-co-(4-acrylamidophenyl) boronic acid) (GO-PAPB) [10], and covalent bonding, for example GO-Borate [1], GO-10, 12-pentacosadiyn-1-ol (GO-PCDO) [11], GO-polyallyl-amine (GO-PAA) [12], GO-poly (dopamine) (GO-PDA) [13], etc. Recently, the synergistic toughening has been demonstrated to be highly effective in enhancing the mechanical performance of graphene-based nanocomposites [14,15], such as the ultrastrong graphene fiber nanocomposites via ionic and covalent bonding [14], ultratough graphene film nanocomposites via hydrogen and covalent bonding [15], etc. Recently, other high performance nacre-mimetic composites have also been reported [16–18]. However, to our knowledge, the synergistic interactions of hydrogen and ionic bonding have not been investigated in enhancing the mechanical performance of graphene-based bioinspired nanocomposites yet.

In this study, we demonstrated the synergistic effect from

*Corresponding author (email: cheng@buaa.edu.cn)
†These authors contributed equally to this work

interfacial interactions of hydrogen and ionic bonding to improve the strength and toughness of bioinspired graphene-based nanocomposites. The hydrogen bonding network is formed between hydroxypropyl cellulose (HPC) and GO nanosheets, then, the ionic bonding is further introduced through copper ions, which results in synergistic effect. The tensile strength of bioinspired nanocomposits reaches 274.3 MPa and the toughness reaches 6.7 MJ/m^3. In addition, this kind of bioinspired nanocomposites show high electrical conductivity with 127.7 S/cm and excellent fatigue-resistant properties. This kind of bioinspired graphene-based nanocomposites may have many latent applications in different aspects, such as flexible electronics devices, aerospace, etc. This bioinspired strategy also opens a door to fabricate excellent mechanical performance bioinspired graphene-based nanocomposites in the future.

2 Experimental

2.1 Experimental section

Materials: Crystalline graphite powder was bought from Qingdao JingRiLai graphite co., Ltd. Hydroxypropyl cellulose (HPC) with average M_w~80,000, were bought from Sigma-Aldrich. The copper(II) chloride –99.999% trace metals basis and hydroiodic acid (HI, 57 wt%) were bought from Sigma-Aldrich.

Fabrication of GO-HPC hybrid layered materials: GO was obtained by the modified Hummers' method. A certain amount of GO nanosheets were dissolved in deionized water with sustaining agitation and ultrasonication. And after that the homogenous GO solution was obtained. The HPC dispersion solution was dropwise put into the GO solution under continuous ultrasonication. Finally, the mixture solution of GO/HPC was transferred to a plastic container into an oven with the temperature of 40°C. The GO-HPC hybrid layered materials were obtained after evaporation for almost 2 d. After HI reduction, the rGO-HPC bioinspired nanocomposite was achieved. The GO-Cu hybrid layered materials were fabricated under the similar process.

Fabrication of GO-HPC-Cu nanocomposites: The HPC and Cu ions solution were dropwise put into the GO solution with different contents and with sustaining agitation and ultrasonication to obtain the homogeneous solution. Finally, the mixture solution of GO/HPC/Cu was assembled into GO-HPC-Cu ternary layered materials by means of similar evaporation process. The rGO-HPC-Cu bioinspired nanocomposites were obtained after HI reduction.

Characterization: The Shimadzu AGS-X Tester with gauge length of 5 mm and loading rate of 1 mm/min was utilized to conduct the tensile testing, and the toughness is calculated from area under stress-strain curves. The samples were cut into strips with a length of 10 mm and width of 3 mm. The final mechanical properties are obtained by averaging 10 specimens. The Instron ElectroPuls E1000 test facility with a frequency of 1 Hz proceed the tensile fatigue tests. Use Quanta 250 FEG and JSM-7500F to get scanning electron microscopy (SEM) images. The thermogravimetric analysis (TGA) was conducted on NETZSCH STA449F3 under nitrogen with a temperature rising rate of 10°C/min from room temperature to 800°C. Fourier transform infrared spectroscopy (FTIR) was collected using a Thermo Nicolet Nexus470 FTIR instrument. The X-ray photoelectron spectroscopy (XPS) measurements were taken in an ESCA-Lab220i-XL (Thermo Scientific) using a monochromatic Al-Ka X-ray source. X-ray diffraction (XRD) was collected from Shimadzu LabX XRD-6000. The electrical conductivities of the hybrid layered materials were measured by a standard two-probe method using a source meter (Agilent E4980A). Raman spectroscopy measurements were conducted by a LabRAM HR800 (Horiba Jobin Yvon) with the excitation energy of 2.54 eV (488 nm). UV-Vis absorption spectra were performed on a Shimadzu spectrophotometer (Model UV-3600, Hitachi, Japan).

2.2 Fabrication of bioinspired nanocomposites

Figure 1(a) is the schematic illustration of fabrication process. GO nanosheets, obtained by the Hummer's method, were mixed with HPC and Cu ions into deionized water. After continuous ultrasonication, the mixed solution was assembled into GO-based layered nanocomposites (GO-HPC-Cu) through an evaporation process [13]. After chemical reduction of hydroiodic acid (HI), the residual functional groups on GO nanosheets were removed and the bioinspired nanocomposites of reduced GO (rGO)-HPC-Cu were obtained, as shown in Figure 1(b). The orderly layered structure of rGO-HPC-Cu nanocomposite is shown in scanning electron microscope (SEM) image of Figure 1(c), and the corresponding energy dispersive X-ray spectroscopy (EDS) image and spectrum of the Cu element originating from $CuCl_2$, reveals that Cu ions are homogeneously distributed without aggregation (Figure 1(d) and (e)). To optimize the ratio of GO to HPC and Cu, the GO-HPC and GO-Cu binary materials were also fabricated through same evaporation process. Four different loadings of GO to HPC (99:1, 97:3, 95:5, and 93:7) were set and the matching binary materials were named as GO-HPC-I, GO-HPC-II, GO-HPC-III, and GO-HPC-IV, respectively. The optimized maximum mechanical properties are achieved for GO-HPC-II. The hybrid layered materials of GO-Cu with different weight ratios (GO:Cu = 99.5:0.5, 99.1:0.9, 98.5:1.5, 98:2 and 97:3) were fabricated and named as GO-Cu-I, GO-Cu-II, GO-Cu-III, GO-Cu-IV, and GO-Cu-V, respectively. For the bioinspired nanocomposites, based on optimized GO-HPC-II, five different weight ratios of GO:Cu (99.5:0.5, 99.1:0.9, 98.5:1.5, 98:2 and 97:3) were fabricated and named as GO-HPC-Cu-I, GO-HPC-Cu-II, GO-HPC-Cu-III, GO-HPC-Cu-IV, and GO-HPC-Cu-V,

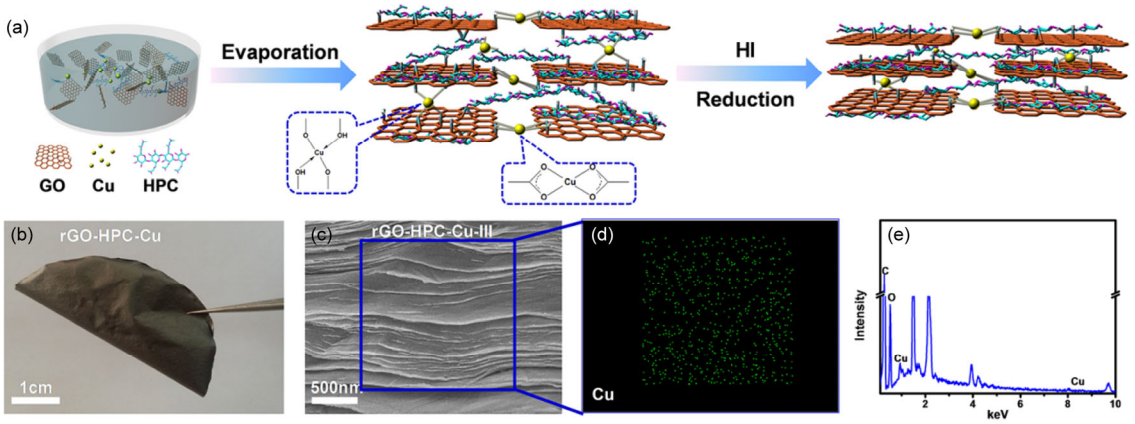

Figure 1 (Color online) (a) Schematic diagram for evaporation self-assembly way to prepare the rGO-HPC-Cu bioinspired nanocomposite; (b) the digital photograph of rGO-HPC-Cu bioinspired nanocomposites; (c) the cross-section of rGO-HPC-Cu bioinspired nanocomposites; (d) matching the Cu element traces from $CuCl_2$ in rGO-HPC-Cu; (e) the EDS spectrum of complete element distribution of rGO-HPC-Cu.

respectively. The exact contents of GO in the resultant nanocomposites were determined via thermogravimetric analysis (TGA), which are displayed in Figure S1, Tables S1 and S2.

2.3 Characterizations and analysis

The interlayer distances (d-spacing) are characterized via X-ray diffraction (XRD) spectrum, which are displayed in Figures 2(a) and S2, indicating that the HPC molecules and Cu were successfully inserted into the interlayers of GO nanosheets. And the d-spacing values of GO-HPC, GO-Cu, GO-HPC-Cu nanocomposites are listed in Tables S3–S5, respectively. After HI reduction, the d-spacing of resultant materials are obviously decreased because of the removal of the residual chemical groups on the surface of GO nanosheets [12]. Fourier transform infrared spectroscopy (FTIR) is aimed to confirm the interfacial interactions between GO nanosheets and HPC or Cu via hydrogen and ionic bonding, as shown in Figure 2(b). Compared to pure HPC film, the –OH stretching peak region (3448 cm^{-1}) and –C-OH peak region (1060 cm^{-1}) shifted to lower wave numbers, the –C-OH peak region shifts from 1085 cm^{-1} for pure HPC thin film, 1058 cm^{-1} for GO-HPC nanocomposites to 1060 cm^{-1} for GO-HPC-Cu nanocomposites, indicating the oxygen-contained functional groups on the surface of GO and the –OH of the HPC molecules form hydrogen bondings [19]. On the other hand, the ionic bonding between carboxylic acid and Cu is confirmed by the increasement of carboxy C-O stretch intensities around 1400 cm^{-1}, the carboxy C-O stretch at 1400 cm^{-1} for GO film, the peak of GO-Cu at 1363 cm^{-1}, and 1378 cm^{-1} for GO-HPC-Cu nanocomposites, shifted to lower wave numbers and decreasement of C=O stretch intensities at 1725 cm^{-1}, indicating ionic bonding between Cu and GO, which are well consistent with previous report [7,20].

Furthermore, the UV-visible transmittance spectroscopy (UV-Vis) absorbance spectra shows the peak shifting from 230 to 233 nm (Figure 2(c)), which is another evidence of the Cu conjugation to GO [20,21]. The X-ray photoelectron spectra (XPS) shows that the C 1s decreased constituent for epoxy/ether group and increased constituent for hydroxyl/alkoxide (Figure 2(d)), compared with pure GO film (Figure S3), indicating the epoxides groups occur ring-opening reaction [7,22]. The ratio of O 1s to C 1s significantly decreased after HI reduction, which means that the residual groups on the GO nanosheets have been removed (Figure S3). Figure 2(e) is the Cu 2p XPS spectra of GO-HPC-Cu, showed typical peaks of Cu^{2+}, that is to say peak at 935.27 eV is assigned core features and peaks at 940.3 and 943.7 eV are assigned to Cu^{2+} satellite line. And also the peak of Binding Energy is less than 932 eV, indicating the existence of Cu^{+} species [23–25]. After HI reduction, the Cu^{2+} turn to Cu^{+} in composites from the bottom of Figure S3. The Raman spectra (Figure 2(f)) indicates the I_D/I_G ratio increases from 1.58 for pure GO film to 1.67 for GO-Cu, 1.64 for GO-HPC, and 1.66 for GO-HPC-Cu. The increasing numerical value of I_D/I_G means new defects induced by copper ion and HPC molecule [26]. Figure S4 shows the same trend for the resultant nanocomposites after HI reduction, and the numerical values are exhibited in Table S6.

3 Results and discussion

The stress-strain curves of the resultant samples were exhibited in Figure 3(a) (the detailed information are shown in Figure S5). The tensile strength of pure GO films reaches 103.1 ± 3.1 MPa and toughness reaches 1.1 ± 0.01 MJ/m^3. After chemically reduced by HI, the tensile strength of rGO films reaches 137.4 ± 5.1 MPa and toughness reaches 1.8 ±

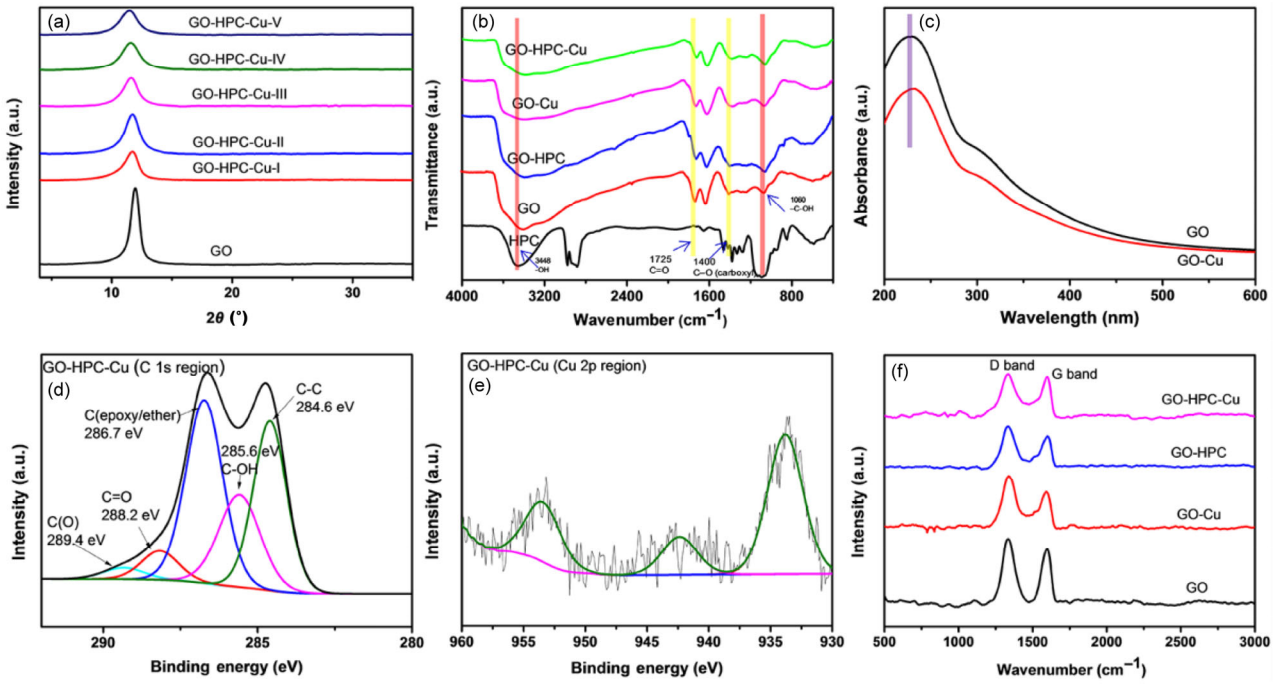

Figure 2 (Color online) (a) XRD of pure GO films, and the GO-HPC-Cu nanocomposites films with different GO contents; (b) FTIR spectra of pure HPC, GO film, GO-HPC film, GO-Cu hybrid materials, and GO-HPC-Cu nanocomposites; (c) UV-Vis absorption spectra of GO and GO-Cu; (d) XPS spectrum of the GO-HPC-Cu nanocomposites; (e) XPS spectrum of Cu 2p region in the GO-HPC-Cu nanocomposites; (f) Raman spectra of GO film, GO-HPC hybrid materials, GO-Cu hybrid materials, and GO-HPC-Cu nanocomposites.

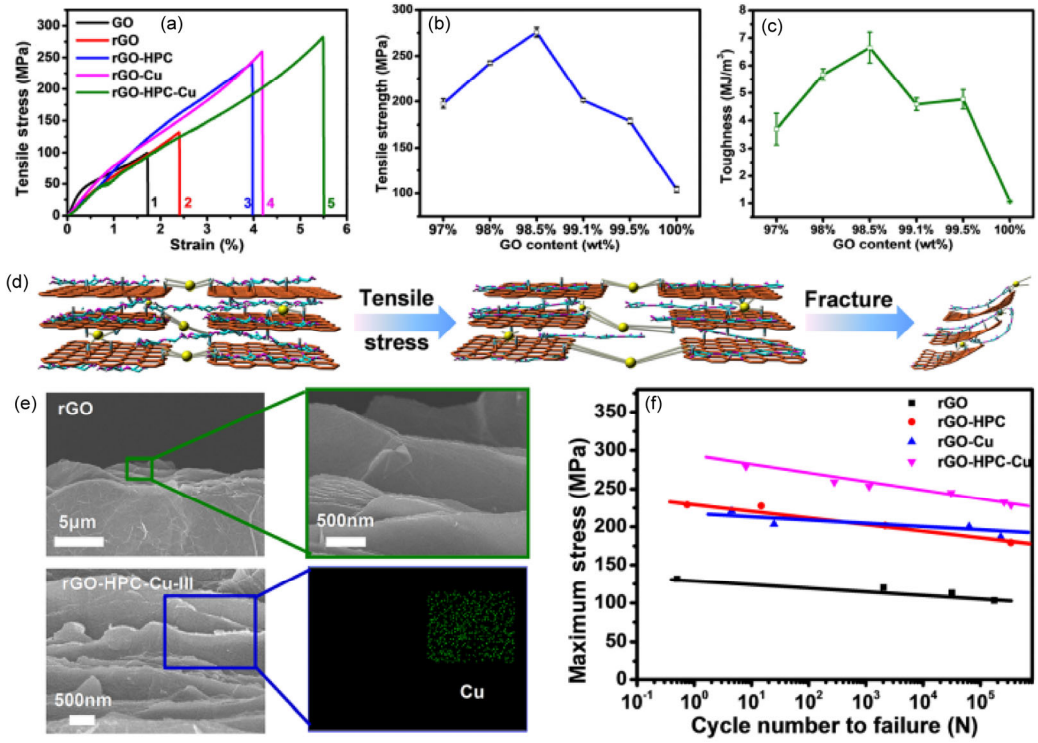

Figure 3 (Color online) (a) The stress-strain curves of GO film (Curve 1), rGO film (Curve 2), rGO-HPC hybrid materials (Curve 3), rGO-Cu hybrid materials (Curve 4), rGO-HPC-Cu nanocomposites (Curve 5); (b) the tensile strength of rGO-HPC-Cu with different GO loadings; (c) the toughness of rGO-HPC-Cu with different GO loadings; (d) the proposed fracture mechanism of rGO-HPC-Cu bioinspired nanocomposite under stress; (e) the side view fracture morphology of rGO and rGO-HPC-Cu bioinspired nanocomposites after tensile testing; (f) the maximum tensile stress versus the number of cycle-times to failure the pure rGO film, rGO-HPC hybrid materials, rGO-Cu hybrid materials, and rGO-HPC-Cu nanocomposites.

0.2 MJ/m^3. When the GO loadings changing, the tensile strength and toughness of bioinspired nanocomposites changing trends are shown in Figure 3(b) and (c), and the numerical values of strength and toughness are shown in the Table S7. The maximum strength of rGO-HPC-Cu-III nanocomposites reaches 274.3 ± 8.7 MPa and toughness reaches 6.7 ± 0.6 MJ/m^3. There is an optimal ratio of HPC to Cu for enhancing the mechanical properties of resultant bioinspired nanocomposites.

When stretching, the hydrogen bonding network between HPC and GO nanosheets were destroyed, and the coiled HPC chain was stretched, then the ionic bonding between Cu and GO nanosheets further fractured. Meanwhile, the hydrogen bonding can also be reformed due to the long chain of HPC, and completely fracture until the breakage of bioinspired nanocomposites. Figure 3(d) exhibits proposed fracture mechanism. Compared with the brittle fracture morphology of pure rGO films (Figure 3(c)), the rGO nanosheets of bioinspired nanocomposites are pull-out and curled at the end of edge. The EDS was performed on the surface of pull-out rGO nanosheets, and the results of EDS showed that the element Cu was uniformly distributing (Figures 3(e) and S6), meaning the friction occurring to rGO nanosheets and Cu in the fracture course. Other nanocomposites have the same fracture morphology, speculating front and side fracture morphology, as shown in Figures S7–S9. This kind of synergistic effect from hydrogen and ionic bonding is superior to previously proposed synergistic effect from building blocks, such as GO nanosheets and montmorillonite (MMT) [27], rGO nanosheets and molybdenum disulfide (MoS_2) [28].

The synergy percentage (S) is utilized to quantify the improvement in mechanical properties of bioinspired nanocomposites induced by synergistic effect [29], which is modified as follows [30]:

$$S = \frac{2\sigma_{\text{hyb}} - (\sigma_{\text{HPC}} + \sigma_{\text{GO}})}{\sigma_{\text{HPC}} + \sigma_{\text{GO}}} \times 100\%,$$

where σ_{hyb}, σ_{HPC}, and σ_{GO} represent the tensile strength of GO-HPC-Cu nanocomposites, GO-HPC binary nanocomposites, and GO film, respectively. The synergy percentage of GO-HPC, GO-HPC-Cu, rGO-HPC-Cu for tensile strength are listed in Table S7. As the exhibition of Figure S10, the synergy percentage of rGO-HPC-Cu-III bioinspired nanocomposites reaches maximum value of 331%, indicating that the optimal ratio of hydrogen bonding and ionic bonding could maximize the synergistic effect.

On the other hand, the synergistic effect from hydrogen and ionic bonding not only enhances the static mechanical properties, but also improves the dynamic mechanical properties, for example, the fatigue-resistant properties. Figure 3(f) shows the maximal tensile stress versus the amount of cycles to failure for pure rGO films, rGO-HPC hybrid materials, rGO-Cu hybrid materials, and rGO-HPC-Cu nanocomposites. The matching stress-strain fatigue curves were shown in Figure S11. For the same stress level, the fatigue life of rGO-HPC binary nanocomposites are comparable to rGO-Cu hybrid materials, but far lower than that of rGO-HPC-Cu bioinspired nanocomposites, further verifying the synergistic effect from hydrogen bonding and ionic bonding. The crack propagation is suppressed by the bridging of HPC via hydrogen bonding and deflected by ionic bonding. Both two crack suppression mechanisms act synergistically, resulting in dissipation of much more energy and prolonging fatigue life.

Compared with the nacre [31] and other rGO-based nanocomposites with single interfacial interaction of hydrogen bonding or ionic bonding, the rGO-HPC-Cu bioinspired nanocomposites with synergistic effect of hydrogen and ionic bonding shows much higher mechanical properties, as shown in Figure 4. The typical GO-based nanocomposites with hydrogen bonding are presented as blue circle, including GO-PVA [6], and rGO-PVA [6], GO-SL [4] and rGO-SL [4], and GO-PMMA [3]. The green square represents the GO-based nanocomposites with ionic bonding, such as, GO-Mg^{2+} [7], GO-Ca^{2+} [7], GO-Fe^{3+}-tannic acid (TA) [32], GO-Al^{3+} [8], and GO-Mg^{2+}-polyimide (PI) [33], respectively. And the mixture of blue and green are the bioinspired nanocomposites with synergistic interfacial interactions of hydrogen and ionic bonding. Obviously, the hydrogen bonding network is only better for enhancing the tensile strength, for example, rGO-SL [4], and the ionic bonding demonstrates high toughness in the GO-Mg^{2+}-PI nanocomposites [33]. The bioinspired nanocomposites show higher strength and toughness, evenly higher than some GO-based bioinspired nanocomposites combining with covalent bonding (the triangle), and synergistic building blocks, for example, GO-PCDO [11], GO-MMT-PVA [27], GO-MoS_2-TPU [28], etc. The numerical values of mechanical properties of nacre and other GO-based nanocomposites

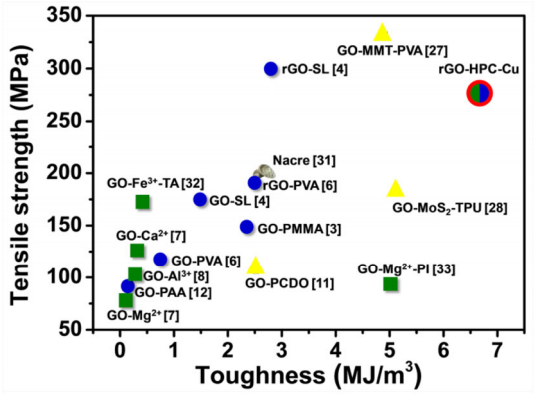

Figure 4 (Color online) The contrast of mechanical properties of bioinspired nanocomposites with other GO-based nanocomposites cross-linked with hydrogen bonding (circle), ionic bonding (square), and covalent bonding (triangle). The results demonstrate that the synergistic effect from hydrogen and ionic bonding is better for enhancing the mechanical properties than single interfacial interaction.

are exhibited in Table S8. Although this kind of bioinspired nanocomposites with synergistic interactions of hydrogen and ionic bonding show relative lower mechanical properties than that of other GO-based nanocomposites with synergistic toughening, such as GO-chitosan [15], GO-cellulose nanocrystal [34], GO-PAPB [10], etc. This study successfully demonstrates the key role of synergistic effect from interfacial interactions about the hydrogen and ionic bonding on simultaneously improving the tensile strength and toughness. Furthermore, the electrical conductivity of bioinspired nanocomposites reaches as high as 127.6 ± 27.2 S/cm for rGO-HPC-Cu-II nanocomposite. Although the addition of HPC molecule would result in the conductivity decreasing of rGO-HPC hybrid materials, the ionic bonding of Cu facilities the resultant electrical conductivity, thus, the electrical conductivity of bioinspired nanocomposites is enhanced.

4 Conclusions

In conclusion, we demonstrated that the synergistic effect from hydrogen and ionic bonding works well for improving the mechanical properties of graphene-based nanocomposites. In particular, the tensile strength and toughness of bioinspired nanocomposites are simultaneously enhanced, as well as high fatigue life. Meanwhile, the electrical conductivity is also improved. This study successfully demonstrates the efficient toughening via constructing synergistic effect from hydrogen and ionic bonding, as well opening a door for constructing excellent performance bioinspired graphene-based nanocomposites, which can be utilized in the application of aerospace, flexible electronics devices, etc.

Supporting Information

The supporting information is available online at tech.scichina.com and www.springerlink.com. The supporting materials are published as submitted, without typesetting or editing. The responsibility for scientific accuracy and content remains entirely with the authors.

This work was supported by the Excellent Young Scientist Foundation of NSFC (Grant No. 51522301), the National Natural Science Foundation of China (Grant Nos. 21273017 & 51103004), Program for New Century Excellent Talents in University (Grant No. NCET-12-0034), Beijing Nova Program (Grant No. Z121103002512020), Fok Ying-Tong Education Foundation (Grant No. 141045), Open Project of Beijing National Laboratory for Molecular Sciences, the 111 Project (Grant No. B14009), Aeronautical Science Foundation of China (Grant Nos. 20145251035 & 2015ZF21009), State Key Laboratory for Modification of Chemical Fibers and Polymer Materials, Donghua University (Grant No. LK1508), the Key Research Program of the Chinese Academy of Sciences (Grant No. KJZD-EW-M03) and the Fundamental Research Funds for the Central Universities (Grant Nos. YWF-15-HHXY-001 & YWF-16-BJ-J-09).

1 Cheng Q, Jiang L, Tang Z. Bioinspired layered materials with superior mechanical performance. Acc Chem Res, 2014, 47: 1256–1266
2 Cheng Q, Duan J, Zhang Q, et al. Learning from nature: Constructing integrated graphene-based artificial nacre. ACS Nano, 2015, 9: 2231–2234
3 Putz K W, Compton O C, Palmeri M J, et al. High-nanofiller-content graphene oxide–polymer nanocomposites via vacuum-assisted self-assembly. Adv Funct Mater, 2010, 20: 3322–3329
4 Hu K, Tolentino L S, Kulkarni D D, et al. Written-in conductive patterns on robust graphene xxide biopaper by electrochemical microstamping. Angew Chem Int Ed, 2013, 52: 13784–13788
5 Hu K, Gupta M K, Kulkarni D D, et al. Ultra-robust graphene oxide-silk fibroin nanocomposite membranes. Adv Mater, 2013, 25: 2301–2307
6 Li Y Q, Yu T, Yang T Y, et al. Bio-inspired nacre-like composite films based on graphene with superior mechanical, electrical, and biocompatible properties. Adv Mater, 2012, 24: 3426–3431
7 Park S, Lee K S, Bozoklu G, et al. Graphene oxide papers modified by divalent ions—Enhancing mechanical properties via chemical cross-linking. ACS Nano, 2008, 2: 572–578
8 Yeh C N, Raidongia K, Shao J, et al. On the origin of the stability of graphene oxide membranes in water. Nature Chem, 2015, 7: 166–170
9 Zhang J, Xu Y, Cui L, et al. Mechanical properties of graphene films enhanced by homo-telechelic functionalized polymer fillers via π–π stacking interactions. Compos Part A-Appl S, 2015, 71: 1–8
10 Zhang M, Huang L, Chen J, et al. Ultratough, Ultrastrong, and Highly Conductive Graphene Films with Arbitrary Sizes. Adv Mater, 2014, 26: 7588–7592
11 Cheng Q, Wu M, Li M, et al. Ultratough artificial nacre based on conjugated cross-linked graphene oxide. Angew Chem, 2013, 125: 3838–3843
12 Park S, Dikin D A, Nguyen S T, et al. Graphene oxide sheets chemically cross-linked by polyallylamine. J Phys Chem C, 2009, 113: 15801–15804
13 Cui W, Li M, Liu J, et al. A strong integrated strength and toughness artificial nacre based on dopamine cross-linked graphene oxide. ACS Nano, 2014, 8: 9511–9517
14 Zhang Y, Li Y, Ming P, et al. Ultrastrong bioinspired graphene-based fibers via synergistic toughening. Adv Mater, 2016, 28: 2834–2839
15 Wan S, Peng J, Li Y, et al. Use of synergistic interactions to fabricate strong, tough, and conductive artificial nacre based on graphene oxide and chitosan. ACS Nano, 2015, 9: 9830–9836
16 Bai H, Chen Y, Delattre B, et al. Bioinspired large-scale aligned porous materials assembled with dual temperature gradients. Sci Adv, 2015, 1: e1500849
17 Bai H, Walsh F, Gludovatz B, et al. Bioinspired hydroxyapatite/poly (methyl methacrylate) composite with a nacre-mimetic architecture by a bidirectional freezing method. Adv Mater, 2016, 28: 50–56
18 Zhao H, Yue Y, Guo L, et al. Cloning nacre's 3D interlocking skeleton in engineering composites to achieve exceptional mechanical properties. Adv Mater, 2016, 28: 5099–5105
19 Ma L, Wang L, Wu L, et al. Cellulosic nanocomposite membranes from hydroxypropyl cellulose reinforced by cellulose nanocrystals. Cellulose, 2014, 21: 4443–4454
20 Mathesh M, Liu J, Nam N D, et al. Facile synthesis of graphene oxide hybrids bridged by copper ions for increased conductivity. J Mater Chem C, 2013, 1: 3084–3090
21 Holler F J, Skoog D A, Crouch S R. Principles of Instrumental Analysis. Belmont: Thomson, 2007
22 Moulder J, Stickle W, Sobol P, et al. Handbook of X-ray Photoelectron Spectroscopy. Eden Prairie: Physical Electronics, 1995
23 Yu X Y, Xu R X, Gao C, et al. Novel 3D hierarchical cotton-candy-like CuO: Surfactant-free solvothermal synthesis and application in As (III) removal. ACS Appl Mat Inter, 2012, 4: 1954–1962
24 Chai L, Wang T, Zhang L, et al. A Cu–m-phenylenediamine complex

induced route to fabricate poly (m-phenylenediamine)/reduced graphene oxide hydrogel and its adsorption application. Carbon, 2015, 81: 748–757

25 Liu P, Hensen E J. Highly efficient and robust Au/$MgCuCr_2O_4$ catalyst for gas-phase oxidation of ethanol to acetaldehyde. J Am Chem Soc, 2013, 135: 14032–14035

26 Hwang J, Yoon T, Jin S H, et al. Enhanced mechanical properties of graphene/copper nanocomposites using a molecular-level mixing process. Adv Mater, 2013, 25: 6724–6729

27 Ming P, Song Z, Gong S, et al. Nacre-inspired integrated nanocomposites with fire retardant properties by graphene oxide and montmorillonite. J Mater Chem A, 2015, 3: 21194–21200

28 Wan S, Li Y, Peng J, et al. Synergistic toughening of graphene oxide—Molybdenum disulfide-thermoplastic polyurethane ternary artificial nacre. ACS Nano, 2015, 9: 708–714

29 Prasad K E, Das B, Maitra U, et al. Extraordinary synergy in the mechanical properties of polymer matrix composites reinforced with 2 nanocarbons. Proc Natl Acad Sci USA, 2009, 106: 13186–13189

30 Dichiara A B, Sherwood T J, Bentonsmith J, et al. Free-standing carbon nanotube/graphene hybrid papers as next generation adsorbents. Nanoscale, 2014, 6: 6322–6327

31 Meyers M A, Chen P Y. Structural biological materials: Critical mechanics-materials connections. Science, 2013, 339: 773–779

32 Liu R Y, Xu A W. Byssal threads inspired ionic cross-linked nacre-like graphene oxide paper with superior mechanical strength. RSC Adv, 2014, 4: 40390–40395

33 Kong J Y, Choi M C, Kim G Y, et al. Preparation and properties of polyimide/graphene oxide nanocomposite films with Mg ion crosslinker. Eur Polym J, 2012, 48: 1394–1405

34 Xiong R, Hu K, Grant A M, et al. Ultrarobust transparent cellulose nanocrystal-graphene membranes with high electrical conductivity. Adv Mater, 2015, 28: 1501–1509